Inelastic-neutron-scattering studies on glassy and liquid $Ca_{0.4}K_{0.6}(NO_3)_{1.4}$

E. Kartini*
Department of Physics and Astronomy, McMaster University, Hamilton, Ontario, Canada L8S 4M1 and Berlin Neutron Scattering Center, Hahn Meitner Institut, Glienickerstrasse 100, D-14109 Berlin, Germany†

M. F. Collins and B. Collier
Department of Physics and Astronomy, McMaster University, Hamilton, Ontario, Canada L8S 4M1

F. Mezei
Berlin Neutron Scattering Center, Hahn Meitner Institut, Glienickerstrasse 100, D-14109 Berlin, Germany

E. C. Svensson
AECL, Chalk River Laboratories, Chalk River, Ontario, Canada K0J 1J0
(Received 30 August 1995; revised manuscript received 22 December 1995)

Triple-axis inelastic-neutron-scattering measurements have been carried out on the ionic glass material $Ca_{0.4}K_{0.6}(NO_3)_{1.4}$. Our measurements of the temperature dependence of the position of the main elastic diffraction peak in the liquid give a linear coefficient of thermal expansion of $(2.3\pm0.2)\times10^{-4}$, which is markedly greater than the value of 1.2×10^{-4} from density measurements. This shows that the expansion is accompanied by structural rearrangements. The Debye-Waller factor, as determined from the temperature dependence of the intensity of the main elastic diffraction peak, shows an anomaly at the calorimetric glass transition temperature, $T_g = 335$ K, but the anomaly at the critical temperature T_c predicted by mode-coupling theory is not seen. In contrast, the change in the effective root-mean-square displacement, $\langle r^2\rangle_T^{\rm eff}-\langle r^2\rangle_{300}^{\rm eff}$ deduced from the Q dependence of the temperature variation of the quasielastic scattering over a wide range of wave vector Q from 2 to 4 Å^{-1}, shows a break of slope at a temperature that can be identified as T_c, but there is no anomaly at T_g. Our results give $T_c = 368 \pm 5$ K. The inelastic scattering for constant Q scans at frequencies $\nu = \omega/2\pi \leqslant 0.5$ THz deviates from harmonic-phonon-like behavior at temperatures above T_g. This can be identified as a fast relaxation or β process, as predicted by mode-coupling theory. Such a deviation is not observed at higher frequencies. In the present work, we establish the Q and ν dependences of the β process. [S0163-1829(96)01230-1]

I. INTRODUCTION

An approach to the glass-transition problem arose when mode-coupling theory (MCT) provided a framework that allows one to calculate the evolution of time correlations from a nonlinear microscopic equation of motion (for a review, see Ref. 1). MCT of atomic supercooled simple liquids predicts the existence of a dynamic instability at some temperature T_c above the glass transition temperature T_g. There are two relaxation steps, identified as primary or α relaxation and secondary or β relaxation. In MCT, T_c is identified by the divergence of the characteristic relaxation times of the α process on cooling, so that only the β process is activated below T_c. The α and β relaxations are governed by different scaling frequencies, with the α process involving the lower frequency. The MCT predictions are formulated in terms of the density-correlation function $\Phi_Q(t)$ and its decay with time. Neutron scattering is a powerful technique to test the predictions of mode-coupling theory, because the scattering function $S(Q,\omega)$ determined by the neutron-scattering measurements is closely related to the Fourier transform of Φ_Q(t).

$Ca_{0.4}K_{0.6}(NO_3)_{1.4}$ (CKN) has for many years been a model system for studies of the glass transition. It is a remarkably stable ionic glass system, which is characterized by non-Arhennius behavior of the viscosity.[2] The first neutron-scattering studies of the dynamics at the glass transition were performed by Mezei and co-workers[3–5] on CKN using neutron spin-echo and time-of-flight spectroscopy. Their results are compatible with the predictions of mode-coupling theory and give strong indications of the existence of a critical temperature T_c at approximately 30° above the glass-transition temperature $T_g = 335$ K. Moreover, the measurements show the existence of two relaxation processes with two scaling frequencies.[4] In the equilibrium liquid state, the line shape of the α relaxation in the ω domain has been also established.[6] The measurements reported in the present paper are at frequencies too high to observe the α relaxation directly, but they are sensitive to β relaxation.

A prerequisite for the applicability of MCT is a smooth temperature dependence of the static structure factor $S(Q)$, so as to ensure that the glass-transition anomalies are of a purely dynamical nature and do not stem from any structural transition.[1] It has been shown in our previous neutron-diffraction measurements of the structure factor $S(Q)$ that there is indeed a continuous change of the main peak intensity with no sudden jump or discontinuity at any temperature.[7] In the present work we extend the investigation of this material with detailed measurements of the elastic structure factor $S(Q,\omega=0)$ and of the inelastic scattering $S(Q,\omega)$.

The specific predictions of mode-coupling theory regarding the Debye-Waller factor and the dynamic structure factor were a motivation for us to carry out the experiments described in the present paper. Previous work observed the dynamic behavior only at $Q=Q_o$, where Q_o is the peak of the structure factor.[3,4] With the technique of neutron triple-axis spectrometry we investigate different physical regions than in the earlier work on CKN and for several values of Q.[3–7] Specifically, constant-energy and constant-Q scans were used to obtain accurate measurements of the temperature dependence of the elastic scattering $S(Q,\omega=0)$ for the range $0.3<Q<4$ Å^{-1} and of the inelastic scattering $S(Q,\omega)$ for frequencies between 0.2 and 1.8 THz and values of Q between 0.5 and 3.0 Å^{-1}.

In Sec. II of this paper we give theoretical predictions for the Q and T dependence of the Debye-Waller factor. In Sec. III we present experimental details, and in Sec. IV describe data for $S(Q,\omega=0)$ and for the inelastic scattering. Section V contains conclusions.

II. DEBYE-WALLER FACTOR

In the glass phase the neutron-scattering spectrum consists of an elastic line $S(Q,\omega=0)$ corresponding to the solid structure and an inelastic contribution $S(Q,\omega)$ related to the fast motion of the atoms around their equilibrium position. Under such circumstances one can define the Debye-Waller factor as (neglected the slight expansion of the structure with temperature)

$$S(Q,\omega=0)=e^{-2W}S_o(Q,\omega=0) \tag{1}$$

where $S_o(Q,\omega)$ refers to $T=0$ K. In the simplest approximation

$$e^{-2W}=\exp[-Q^2\langle r^2\rangle/3], \tag{2}$$

where Q is the scattering vector and $\langle r^2\rangle$ is the mean-square displacement of an atom from its average position. In the supercooled liquid phase the elastic structure factor $S(Q,\omega=0)$ is, strictly speaking, zero (onset of the α relaxation), but this process is slow enough so that we can maintain the above definition of the Debye-Waller factor by replacing $\omega=0$ by a condition $|\omega|<\Delta$, where Δ is window determined by a conveniently chosen instrumental resolution function. This means that $\langle r^2\rangle$ is averaged over times of order of the reciprocal of the frequency instrumental resolution function; in the present experiment the resolution is of order 0.1 THz, so the averaging time is of order 10^{-11} s. From previous results[3–6] we know that the α relaxation is confined to times longer than this for the temperatures studied in this work, while the β relaxation occurs at shorter times.

Harmonic phonon theory predicts that $\langle r^2\rangle$ will be directly proportional to the temperature at temperatures where the zero-point motion does not dominate the vibrations. This condition is satisfied at and above room temperature for CKN. If there is a change in the β relaxation at certain temperatures this will be reflected in anomalies in the temperature dependence of the Debye-Waller factor. In particular, it has been predicted from mode-coupling theory[1] that the Debye-Waller factor will contain a term proportional to $(T_c-T)^{1/2}$ for $T_g<T<T_c$.

The Debye-Waller factor is determined from the variation of the elastic scattering $S(Q,\omega=0)$ with temperature. By analogy with crystalline solids, where the temperature dependence of the height of the Bragg peaks determines the Debye-Waller factor, we determine the Debye-Waller factor for CKN from the intensity of the quasielastic peak.

Since $\langle r^2\rangle$ is different for all atomic species in the sample, the effective $\langle r^2\rangle$ in Eq. (2) is an average over these individual terms with weight factor which in general vary with Q. Thus we should expect deviations in the Q dependence of the Debye-Waller factor from the simple Q^2 law.

III. EXPERIMENT

Nitrate glasses were prepared from commercially available reagent-grade nitrates, 99.99% KNO_3 and 99.99% $Ca(NO_3)_2\,4H_2O$. Melting was carried out in a furnace under vacuum, and all other operations were carried out in a glove box with an argon atmosphere. The raw materials were dried before weighing to get precise atomic proportions.

The dried raw materials were mixed together in appropriate proportions and placed in a sealed glass tube. After the temperature was raised to 473 K, the nitrates mixture started to melt. The temperature was then raised in steps of 50, 30, 30, 30, and 40 K, at about hourly intervals, after visible water emission had ceased. At 583 K the mixture became a clear yellowish liquid. The melt was then heated up to 653 K when it became extremely clear. To remove any remaining water, the sample was evacuated under 10^{-5} torr and then was flushed by N_2 gas for a few hours. The melt was poured into an aluminum slab container with dimensions $0.5\times5\times7$ cm^3 for the neutron experiment. The perimeter of the sample container then was masked by boron nitride to give an area of 4 cm high by 6 cm wide. Differential thermal analysis determined the glass-transition temperature T_g to be 335 K. The procedure for making the glass sample was described in detail in a previous paper.[7]

The inelastic-neutron-scattering experiment was performed with the DUALSPEC triple-axis spectrometer at the NRU reactor at the Chalk River Laboratories of AECL. Si(113) and Ge(113) were used as the monochromator and analyzer, respectively. The scattered neutron energy was fixed at 3.52 THz. Sapphire and pyrolitic graphite filters were placed in the incident and scattered beams, respectively, to suppress higher-order neutrons. The resolution at the elastic position was 0.105-THz full width at half maximum (FWHM). The sample was mounted in a furnace in a helium atmosphere. During the measurements the sample was kept in symmetric transmission. The transmission of the sample at normal incidence was 85%. Including both absorbtion and scattering effects, the total scattering is about 10%. No correction for multiple scattering was made in our data evaluation procedure. Measurements were carried out at temperatures between 300 and 573 K, with the sample in either a glass, a supercooled liquid, or a normal liquid state. The scattering from $Ca_{0.4}K_{0.6}(NO_3)_{1.4}$ is almost entirely coherent ($\sigma_{\rm coh}=35.5$ b and $\sigma_{\rm inc}=0.85$ b).

In addition to the measurements of the scattering from

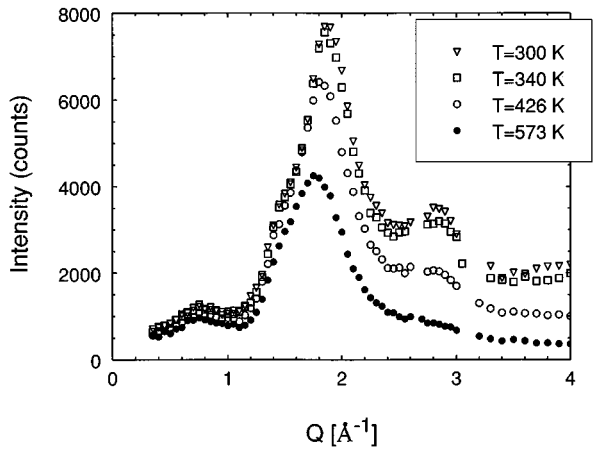

FIG. 1. The elastic scattering intensity $S(Q,\omega=0)$ for $Ca_{0.4}K_{0.6}(NO_3)_{1.4}$ at temperatures of 300, 340, 426, and 573 K, when the system is in glassy, supercooled liquid, supercooled liquid, and liquid states, respectively.

CKN plus the sample holder, we also measured the scattering from an empty sample holder at two temperatures, 300 and 573 K. Accurate determination of $S(Q,\omega=0)$ was not possible where there are powder peaks from the aluminum sample container at Q values of 2.7 and 3.1 Å^{-1}. To correct for the effect of rotating the large flat sample in an inhomogenous flux distribution, beam profiles were determined (by measuring the scattering from a thin polythene rod as it was translated across the incident beam at the sample position) for six values of the monochromator scattering angle $2\theta_m$, covering the range employed for the measurements. As well as the beam profile correction, corrections were made for absorbtion and for the scattering from the empty sample holder.

IV. RESULTS AND DISCUSSIONS

A. Elastic scattering $S(Q,\omega=0)$

The elastic structure factor $S(Q,\omega=0)$ of CKN is shown in Fig. 1, at temperatures of 300, 340, 426, and 573 K, when the system is a glass, a supercooled liquid, a supercooled liquid, and a liquid, respectively. The spectra show features typical of a noncrystalline material, which are generally similar for the glass, supercooled liquid, and liquid phases, but there are systematic changes with temperature.

There are three peaks in $S(Q,\omega=0)$. The first small peak at about 0.8 Å^{-1} corresponds to the nearest cation to cation (or anion to anion) distance, which is the characteristic dynamic length scale of the melt. This peak position does not change with temperature since the strong electrostatic forces tend to stabilize the distance. The second peak at 1.88 Å^{-1} (at room temperature) is the main peak of the structure factor. The third peak is at 2.8 Å^{-1}. Due to the complexity of our glass system (with the NO_3 group as a single anion and two cations), the latter two peaks do not simply correspond to single ionic-pair separation distances but to a combination of several distances between several ionic pairs, i.e., each peak has contributions from several ionic pairs. With increasing temperature, the positions of the latter two peaks shift to lower Q, and their intensities decrease markedly.

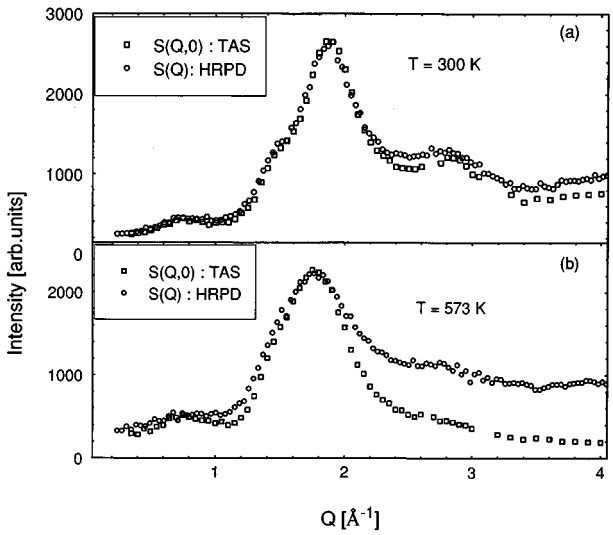

FIG. 2. Comparisons of the static structure factor $S(Q)$ (open circles) measured using a high-resolution powder diffractometer (HRPD) (Ref. 7), and the elastic structure factor $S(Q,\omega=0)$/(open squares) measured using a triple-axis spectrometer (TAS) for temperatures of 300 K (a) and 573 K (b).

The three-peaked pattern of Fig. 1 is also found[7] in the static structure factor $S(Q)$ as measured by neutron diffraction at $\lambda = 1.5$ Å . Comparisons of $S(Q)$ measured[7] using a high-resolution powder diffractometer and our $S(Q,\omega=0)$ measured using a triple-axis spectrometer are shown in Figs. 2(a) and 2(b) for temperatures of 300 and 573 K, respectively. For each temperature, the elastic-scattering data are normalized to give the same height at the main peak as the neutron-diffraction data. Note that there are marked differences between $S(Q)$ and $S(Q,\omega=0)$ at high Q and high temperatures, showing the considerable inelastic contribution to $S(Q)$ in this region.

In this section, we concentrate on the temperature variation of the main peak of $S(Q,\omega=0)$. To quantify its behavior, this peak was fitted with a Gaussian function

$$S_{\text{peak}}(Q,\omega=0,T)=Ae^{[-(Q-Q_o)^2/2\Gamma^2]} \tag{3}$$

for values of Q within about 0.15 Å^{-1} of Q_o, where Q_o is the position of the main peak. Equation (3) includes the temperature dependence of $S(Q,\omega,T)$ explicitly. For much of this paper such explicit inclusion is not necessary, and the function is just written as $S(Q,\omega)$. The fitted parameters are the peak height (A), the peak position (Q_o), and the width (Γ). In all cases, the top of the main peak is fitted reasonably well with such a Gaussian function, as is illustrated in Fig. 3 for temperatures of 320, 350, 370, and 390 K.

Figure 4 shows that the peak position varies linearly with temperature above $T_g = 335$ K. Open circles show the data obtained by heating the sample from room temperature, and open squares show the data obtained by cooling the sample from $T=573$ K. The heating data extend to 390 K, where crystallization commenced. There is no significant difference between the heating and cooling data. From the refractive index data of Rao, Helphrey, and Angell,[8] the density measurements of Dietzel and Poegel[9] and from a previous

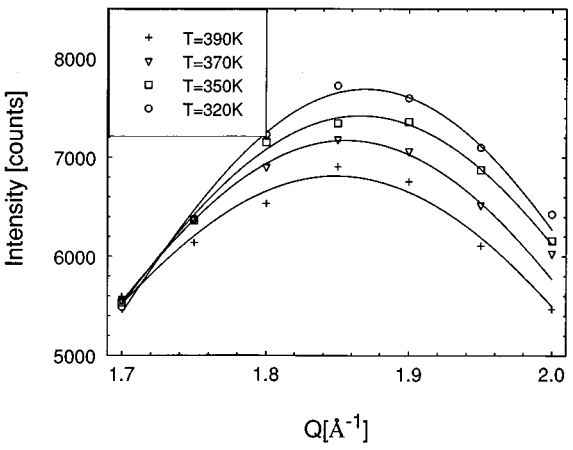

FIG. 3. Gaussian fits of the elastic main peak intensities at 320, 350, 370, and 390 K. From such fits the peak height and peak position were obtained for each temperature.

neutron-diffraction experiment,[7] the linear thermal-expansion coefficients are 1.17×10^{-4}, 1.28×10^{-4}, and $(1.79\pm0.12)\times10^{-4}$, respectively. Our present results give a value of $(2.3\pm0.2)\times10^{-4}$, which is larger than from the other measurements.

The difference between the thermal expansions observed in $S(Q)$ and $S(Q,\omega=0)$ is explained by the presence of an inelastic component in $S(Q)$. It can be quantitatively evaluated by taking into account the observed temperature dependence of the Debye-Waller factor. In fact using the Gaussian linewidth parameter Γ [cf. Eq. (3)] as determined, together with a flat background in Ref. 7 ($\Gamma\simeq 0.2$ Å^{-1}) and the temperature variation of $\langle r^2\rangle^{\rm eff}$ as given below in Fig. 7, we obtain a difference of 0.5×10^{-4}/K for the linear thermal-expansion coefficient for $S(Q,\omega=0)$ and $S(Q)$, respectively, in agreement with measured value.

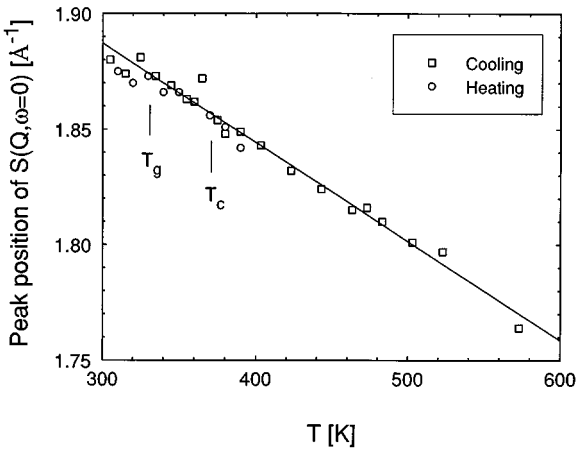

FIG. 4. The temperature dependence of the position of the main peak in $S(Q,\omega=0)$ obtained from Gaussian fitting. The peak position varies linearly with increasing temperature above $T_g=335$ K. The data give a coefficient of linear thermal expansion of 2.3×10^{-4}. There is no change of slope at T_c, but there is some indication of a change at T_g with a lower coefficient of thermal expansion in the glasseous state.

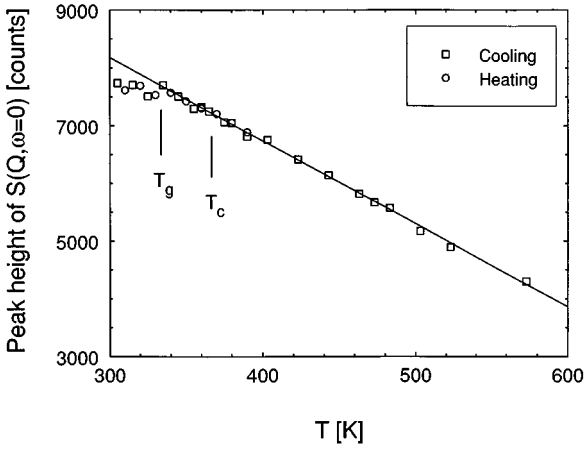

FIG. 5. The temperature dependence of the height of the main peak of $S(Q,\omega=0)$. There is a linear variation for $T>T_g$, with departures at lower temperatures. In contrast to the predictions of mode-coupling theory (Ref. 1), the data do not show a variation with temperature of the form $(T_c-T)^{1/2}$ between T_g and T_c, and show no anomaly at the critical temperature T_c as inferred in a previous work.

The Q^2 background shifts the apparent peak position to higher Q at higher temperature, thus reducing the apparent variation of the peak position with temperature. The neutron-scattering measurements give larger coefficients of thermal expansion than the density measurements. This indicates that there is structural rearrangement as the temperature changes. There is no indication of a change of slope at T_c in Fig. 4, but there is some indication of a change at T_g. This effect has been seen in thermal-expansion data previously,[8] where a smaller expansion coefficient 0.33×10^{-4} was observed in the glass.

We analyzed the Debye-Waller factor characterizing the T and Q dependences of the elastic-quasielastic central line (within the energy resolution, the line is still elastic). Figure 5 shows the temperature dependence of the peak height of $S(Q,\omega=0)$. There is a linear variation for $T>T_g$, with departures at lower temperatures. Following the discussion given in Sec. II, the plot in Fig. 5 is to be interpreted as a plot of the temperature dependence of the Debye-Waller factor. By plotting the peak height rather than the intensity at fixed Q, thermal-expansion effects are allowed for. There is a change in slope at T_g followed by the extra decrease of the elastic intensity above this temperature. The extra decrease above T_g can be identified with the onset of the β relaxation process, as predicted by mode-coupling theory, though the results do not show the square-root behavior at $T_g< T<T_c$ as theory predicts,[1] and there is no anomaly at T_c.

We have determined the Debye-Waller factor at other values of Q from the measured temperature dependence of the elastic scattering $S(Q,\omega=0)$. Normalizing the scattering to its value at 300 K and using Eq. (2), we expect that

$$\ln\left[\frac{S(Q,\omega=0,T)}{S(Q,\omega=0,T=300\ \mathrm{K})}\right]=-Q^2[\langle r^2\rangle_T-\langle r^2\rangle_{300}]/3. \quad (4)$$

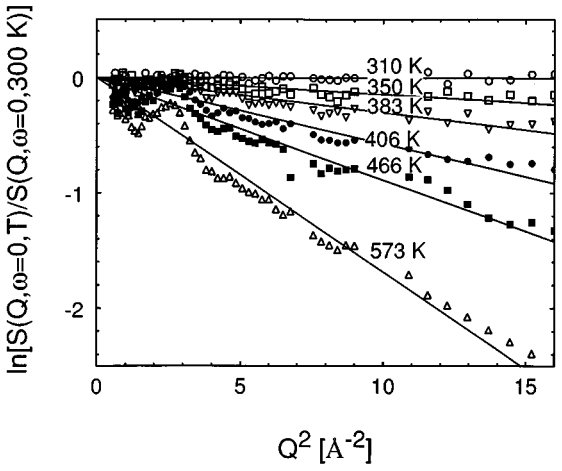

FIG. 6. $\ln[S(Q,\omega=0,T)/S(Q,\omega=0,T=300\ \mathrm{K})]$ plotted against Q^2 in the range of Q from 0.5 to 4 $\mathrm{\AA}^{-1}$. The plots are fitted to a linear function passing through the origin for $Q \geq 2\ \mathrm{\AA}^{-1}$. The slope gives the change in the effective root-mean-square displacement, $\langle r^2\rangle_T^{\mathrm{eff}} - \langle r^2\rangle_{300}^{\mathrm{eff}}$.

Figure 6 shows $\ln[S(Q,\omega=0,T)/S(Q,\omega=0,T=300\ \mathrm{K})]$ plotted against Q^2 for some typical temperatures over the range of Q from 0.5 to 4 $\mathrm{\AA}^{-1}$. We found that a mean square displacement $\langle r^2\rangle$ can only be defined for $Q \geq 2\ \mathrm{\AA}^{-1}$ that is beyond the peak of the structure factor. The slope, which gives a measure of $\langle r^2\rangle_T^{\mathrm{eff}} - \langle r^2\rangle_{300}^{\mathrm{eff}}$, is now primarily determined by larger values of Q than was the case for the fits to the height of the main peak. Here the notation eff or effective means that we only use a value of Q larger than 2 $\mathrm{\AA}^{-1}$, and not for all the range of Q values. The bump around 3 $\mathrm{\AA}^{-2}$ in the data points in Fig. 6 is primarily due to the shift of the position of the peak of the structure factor.

Figure 7 shows the effective root-mean-square displacement $\langle r^2\rangle_T^{\mathrm{eff}} - \langle r^2\rangle_{300}^{\mathrm{eff}}$ obtained from fits to data like those shown in Fig. 6. The T dependence of the effective root-mean-square displacement suggests a discontinuity of slope at temperature T_c with no anomaly at T_g, in contrast to the results shown in Fig. 5, where there is a change in slope at T_g but none at T_c. The accuracy of our data, as also illustrated by the scatter of the points in Fig. 6 (e.g., the straight line fitted in the temperature range 310–370 K deviates from the defined value of 0 at 300 K) is not quite sufficient for making a definitive statement. Nevertheless, it is tempting to identify T_c with the critical temperature of the dynamic phase transition predicted by mode-coupling theory.[1] This suggests a way for a possible direct observation of the mode-coupling critical temperature. In previous work[3–5] this temperature could only be identified tentatively by fitting data with two scaling functions assuming *a priori* the existence of T_c.

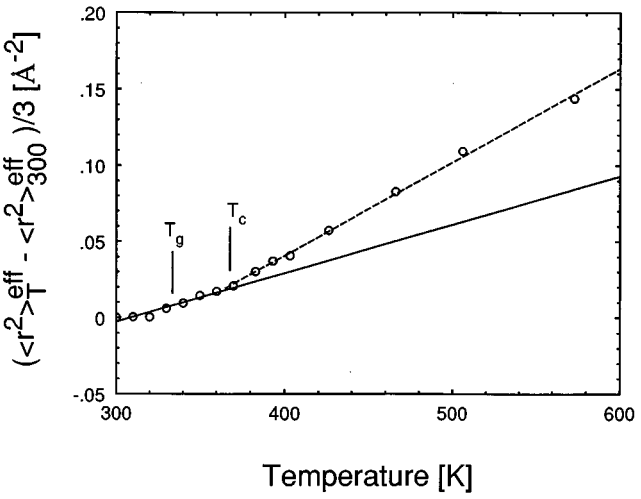

FIG. 7. The change in the effective root-mean-square displacement, $\langle r^2\rangle_T^{\mathrm{eff}} - \langle r^2\rangle_{300}^{\mathrm{eff}}$, as a function of temperature. There is a discontinuity in slope at T_c with no anomaly at T_g. This gives a value of 368 ± 5 K for the critical temperature T_c.

If we fit the data shown in Fig. 7 to two linear functions, we find that $T_c = 368 \pm 5$ K. Earlier neutron time-of-flight and spin-echo measurements[3–5] have given similar values for T_c, 368 ± 5 and 370 ± 5 K, respectively. Contrary to the predictions of mode-coupling theory,[1] the results do not show a variation of the Debye-Waller factor with temperature of the form $(T_c - T)^{1/2}$ between T_g and T_c.

B. Inelastic scattering for constant Q

In order to analyze the temperature behavior of $S(Q,\omega)$ for $\nu \geq 0.2$ THz, we consider the local vibrations of atoms in a liquid or glass as ''phononlike'' motions $S^{\mathrm{ph}}(Q,\omega)$. For the long-wavelength acoustic single-phonon scattering process[10] in the incoherent approximation,

$$S^{\mathrm{ph}}(Q,\omega,T) = \frac{\sigma_{\mathrm{coh}}}{4\pi}\frac{Q^2}{2M\omega}e^{(-Q^2\langle r^2\rangle/3)}S(Q)z(\omega)n_B(\omega,T), \tag{5}$$

where $\langle r^2\rangle$ and $\overline{M}$ are the average effective atomic displacement and atomic mass, respectively, $n_B(\omega,T)$ is the Bose occupation number, and $z(\omega)$ is the density of states. As mentioned in Sec. II, the term $\langle r^2\rangle$ in Eq. (5) can be approximated as $3cT$, where c is a constant. If $Q^2\langle r^2\rangle/3$ is not small compared to 1, there will be a substantial multiphonon contribution, but in the limits $Q \to 0$ and $2W \to 0$, the multiphonon processes become negligible.

We studied the scattering at low frequency to see if this reflects the transitions at T_g and T_c. In this region, $n_B(\omega,T)$ and $z(\omega)$ can be approximated by $k_BT/\hbar\omega$ and ω^2. The single-phonon scattering then becomes

$$S^{\mathrm{ph}}(Q,\omega,T) \propto S(Q)Q^2T, \tag{6}$$

The low-frequency phonon intensity is thus directly proportional to the temperature. We remove the Bose factor from the observed scattering in order to determine the quantity $S_n(Q,\omega,T)$ defined by

$$S_n(Q,\omega,T) = \frac{S^{\mathrm{ph}}(Q,\omega,T)}{n_B(\omega,T)}n_B(\omega,300\ \mathrm{K}) \sim Q^2S(Q). \tag{7}$$

$S_n(Q,\omega,T)$ is thus proportional to $Q^2S(Q)$. Any temperature and frequency dependency of $S_n(Q,\omega,T)$, beyond higher-order effects such as the Debye-Waller factor and

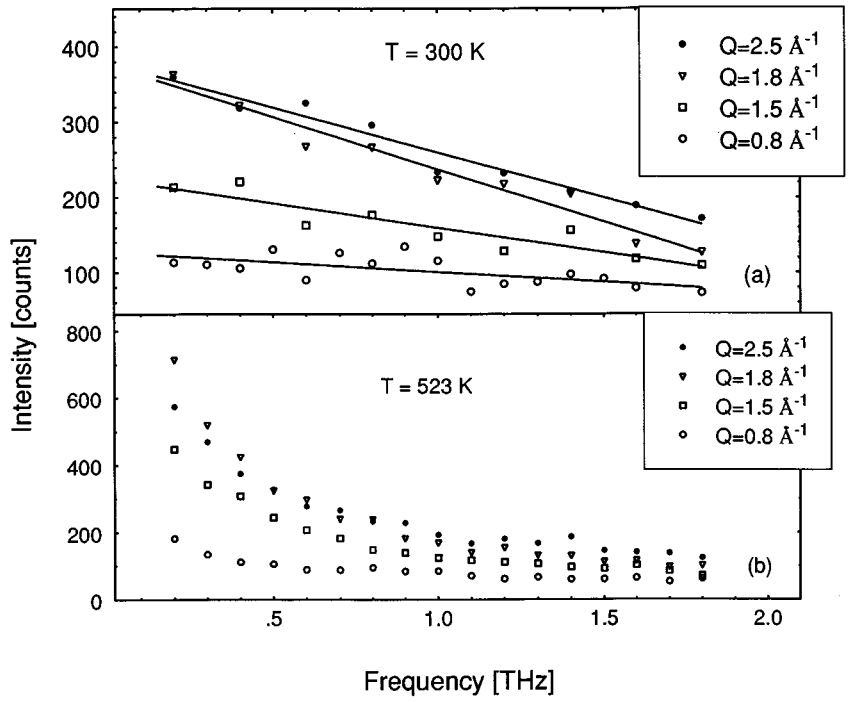

FIG. 8. (a) Room-temperature inelastic constant Q scans at Q values of 0.8, 1.5, 1.8, and 2.5 Å^{-1}. There is an increase of intensity $S_n(Q,\omega,\mathrm{T})$ with increasing Q, and the data are well described by linear fits (solid lines). (b) Constant Q scans for $T=$ 523 K for Q values of 0.8, 1.5, 1.8, and 2.5 Å^{-1}.

normal anharmonicity, reflects a fundamental physical change as the temperature is varied.

$S_n(Q,\omega,T)$ is shown in the range of frequencies from 0.2 to 1.8 THz for constant Q values of 0.8, 1.5, 1.8, and 2.5 Å^{-1}, in Figs. 8(a) and 8(b), at $T=300$ and 523 K, respectively. The major difference between these two plots is the extra intensity at low frequency for $T=523$ K. At higher temperatures, the structural α relaxation induces a broadening of the central quasielastic line. Previous higher resolution time-of-flight measurements at $Q=Q_o$ (Refs. 4 and 6) have shown that this line broadening remains small compared with our resolution width (0.105 THz) over the whole temperature range of the present study. For example, it only amounts to 0.03 THz FWHM at 573 K. In fact we made measurements of the quasielastic scattering over the range from -0.16 to 0.16 THz over the whole range of temperatures and saw no broadening.

To search for possible physical changes near the glass transition in CKN, we determined the frequency and temperature dependences of the quantity $S_n(Q,\omega,T)$ for Q values of 0.8, 1.1, 1.5, 1.8, and 2.5 Å^{-1}. The results show an extra inelastic intensity at temperatures above T_g for frequencies smaller than 0.6 THz, but not for higher frequencies. Similar effects have been shown by the previous time-of-flight results at the main peak of the structure factor $Q_o=1.8$ Å^{-1} in CKN[4] with extra intensity for temperatures above T_g in the frequency range below 0.5 THz.

As we noted above, $S_n(Q,\omega,T)$ is independent of temperature for harmonic phonon scattering. At frequencies below 0.6 THz, $S_n(Q,\omega,T)$ deviates from temperature-independent-behavior for temperatures above T_g. This indicates the onset of a dynamical process at, or very near, the glass-transition temperature, in a frequency range accessible to our measurements. As discussed above, this deviation from the normal phononlike intensity is not caused by broadening of the quasielastic line. The extra intensity must arise from some process that comes into effect for temperatures above T_g at frequencies that are near the low-frequency end of our present measurements but are still much higher than the characteristic frequency of α relaxation.[10] The extra intensity above T_g implies the extra decrease of the Debye-Waller factor above T_g, as described in Sec. IV A. We identify this extra intensity with the β-relaxation process as predicted by mode-coupling theory.[1]

It is interesting to examine the frequency dependence of the extra inelastic intensity. This is shown in Fig. 9 for Q values 0.8, 1.5, and 1.8 Å^{-1} over the range of frequency from 0.2 to 0.8 THz. The intensity was determined by subtracting the temperature-independent intensity for $T<T_g$ from the linearly fitted intensity at 350 K, then normalizing them to the $S(Q,0)$ at temperature 300 K. It is clear that the

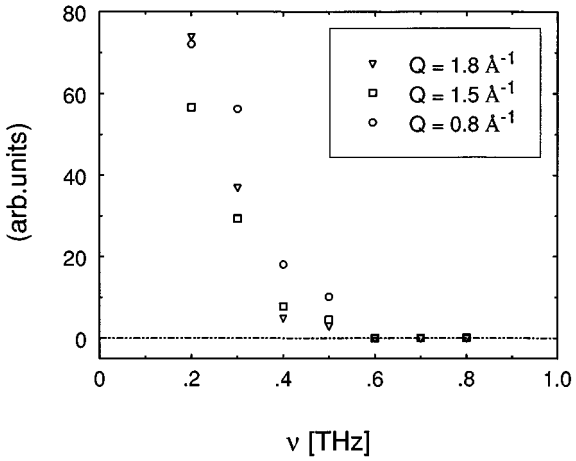

FIG. 9. The frequency dependence of the extra intensity $S'(Q,\omega,T)$ at temperature 350 K for Q values at 0.8, 1.5, and 1.8 Å^{-1}. The data were normalized to the elastic structure factor $S(Q,0)$, at 300 K.

extra intensity decreases markedly with increasing frequency from 0.2 to 0.5 THz, and is absent at higher frequencies. The β relaxation is characterized by the same energy for all the Q values we studied. This is an interesting finding for the coherent scattering. The Q independence of the β process has also been observed in the incoherent scattering [e.g., in orthoterphenyl (Ref. 11)].

We investigated the Q dependence of the β process, since previous work has been confined to the value of Q corresponding to the peak of the structure factor. To determine the Q dependence of the extra intensity at low frequencies, $S'(Q,\omega,T)$, we use a functional form

$$S_n(Q,\omega,T)=\begin{cases} a(Q,\omega)+S'(Q,\omega,T), & T>T_g, \\ a(Q,\omega), & T<T_g, \end{cases} \tag{8}$$

where $a(Q,\omega)$ is the temperature-independent part of $S_n(Q,\omega,T)$. The values of $S'(Q,\omega,T)$ for $\nu=0.2$ THz are plotted in Fig. 10(a). For comparison, $S(Q)$ (Ref. 7) and $S(Q,\omega=0)$ at 360 K are also shown. The general form of $S'(Q,\omega,T)$ is clearly similar to that of $S(Q)$, as predicted by theory.[3] This form is not the same as would be anticipated for acoustic harmonic-phonon scattering, where a behavior like $Q^2S(Q)$ would be expected [Eq. (7)].

We find empirically[10] that

$$S'(Q,\omega,T)\approx b(Q,\omega)S(Q)(T-T_g), \tag{9}$$

where $b(Q,\omega)$ reflects the relative amplitude of the β process. The quantity $b(Q,\omega)$ can be obtained via Eq. (9) from the data shown in Fig. 10(a) at $\nu=0.2$ THz. The results are given in Fig. 10(b). They are consistent with a minimum in the region of the peak of the structure factor as predicted by mode coupling theory.[1,10]

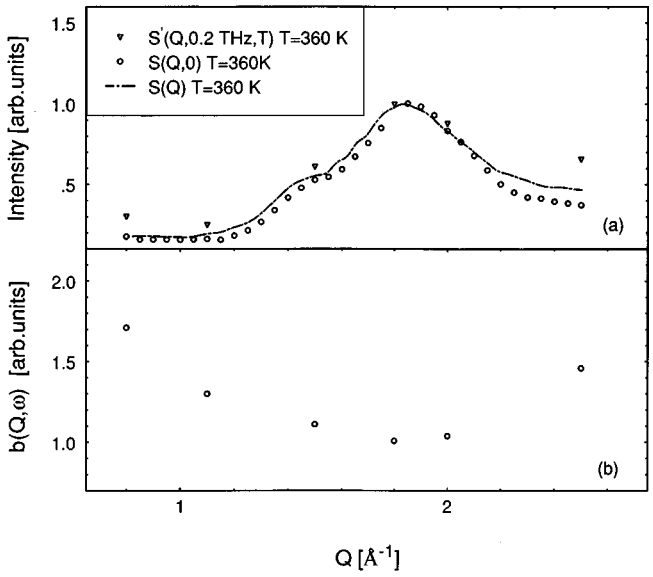

FIG. 10. (a) Triangles show the Q dependence of the magnitude of the extra scattering intensity $S'(Q,\omega,T)$ at temperature 360 K and $\nu=0.2$ THz. For comparison, $S(Q)$ (dashed line) (Ref. 7) and $S(Q,\omega=0)$ (solid line) at 360 K are also shown. (b) The values of $b(Q,\omega)$ obtained via Eq. (9) from the data shown in (a).

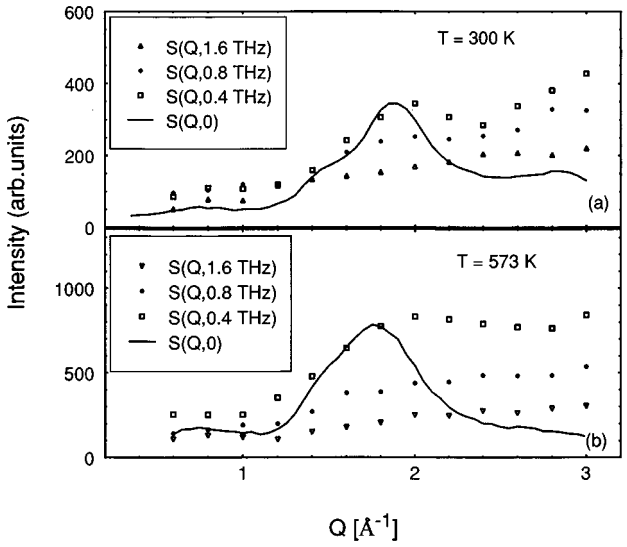

FIG. 11. (a) The inelastic harmonic phononlike scattering at frequencies of 0.4, 0.8, and 1.6 THz in the glassy state (300 K). For comparison, the elastic scattering $S(Q,\omega=0)$ at 300 K in arbitrary units is also shown (solid line). (b) The inelastic scattering at frequencies of 0.4, 0.8, and 1.6 THz in the liquid state (573 K). For comparison, the elastic scattering $S(Q,0)$ at 573 K in arbitrary units is also shown (solid line).

C. Dynamic structure factor at constant ω

In this section we present measurements of the low-frequency inelastic scattering in the glass and liquid states at constant frequency $\nu=\omega/2\pi$. Figure 11 compares $S(Q,\omega=0)$ with $S(Q,\omega)$ for the range of Q from 0.5 to 3 Å^{-1} at frequencies of 0.4, 0.8, and 1.6 THz and temperatures of 300 and 573 K. It is clear that the peak corresponding to the dominant peak of the elastic structure factor is missing in the inelastic scattering. A remnant of this peak is only apparent at the lowest frequency, 0.4 THz. A similar effect has also been observed in vitreous silica.[12] The inelastic scattering at 573 K for a frequency of 0.4 THz is rather flat for $Q>1.8$ Å^{-1}. It does not decrease at large Q like $S(Q,\omega=0)$, and like one would expect if one were observing the tail of a broadened quasielastic component.[13]

Figure 12 shows the inelastic scattering at 0.4 THz, and compares it with $Q^2S(Q)$ and with $Q^2S(Q,\omega=0)$ for temperatures of 300 and 573 K. The data are normalized to give the same height at the main peak. At Q values above the main peak, the results for $\nu=0.4$ THz follow $Q^2S(Q)$, but at smaller Q values they are much greater than the $Q^2S(Q)$ dependence expected for harmonic acoustic phonons. We hypothesize that this extra scattering corresponds to the well-known excess density of low-energy modes in amorphous materials. It is believed that these modes are localized with an extent of a few-nearest-neighbor distances.

V. CONCLUSION

Our experimental results show that the position of the main peak of the elastic scattering $S(Q,\omega=0)$ shifts to

lower Q linearly with increasing temperature in the liquid state ($T > T_g$). There is evidence for a lower coefficient of expansion in the glass state (Fig. 4). Our measured coefficient of linear thermal expansion in the liquid state is 2.3×10^{-4}, which is larger than the values from the refractive index,[8] from the density,[9] and from neutron-diffraction data,[7] which are 1.17×10^{-4}, 1.28×10^{-4}, and 1.79×10^{-4}, respectively. That the neutron-scattering measurements give a larger coefficient of thermal expansion than density measurements is an indication that there are structural rearrangements as the temperature changes. The difference in the value of the coefficient of thermal expansion given by $S(Q,\omega=0)$ and $S(Q)$ can be explained by the inelastic contribution to $S(Q)$, which varies as Q^2T, and shifts the main peak of $S(Q)$ to higher Q at higher temperature. $S(Q)$ clearly reflects the equal-time correlations, i.e., the instantaneous density pattern, better than $S(Q,\omega=0)$ does.

The height of the main peak of the elastic scattering $S(Q,\omega=0)$ shows an anomaly at T_g. As can be seen in Fig. 5, there is a change of slope at T_g. The steeper decrease above T_g is attributed to the onset of a fast relaxation or β process, as predicted by mode-coupling theory, but there is no indication of the anomaly at a critical temperature $T_c > T_g$ expected from mode-coupling theory . In contrast to the predictions of mode-coupling theory,[1] the elastic main peak intensity does not vary with temperature between T_g and T_c like $(T_c - T)^{1/2}$; rather it varies linearly throughout this region and above.

A signature of the expected critical behavior is, however, obtained from the Q dependence of the Debye-Waller factor over the range of Q from $\sim$ 2 to 4 Å^{-1}, while the behavior is more complicated below 2 Å^{-1}. The data in Fig. 6 show that $\ln[S(Q,\omega=0,T)/S(Q,\omega=0,T=300\text{ K})]$ varies linearly with Q^2, for $Q \geqslant 2$ Å^{-1}, the slope giving a measure of the change in the effective root-mean-square displacement, $\langle r^2\rangle_T^{\text{eff}} - \langle r^2\rangle_{300}^{\text{eff}}$, as depicted in Fig. 7. The temperature dependence of the effective root-mean-square displacement breaks at a critical temperature T_c, but not at a glass transition temperature T_g.

The result obtained in Fig. 7 is in contrast to the results for the main peak in $S(Q,\omega=0)$, that shows the discontinuity at T_g (Fig. 5). It remains to be understood why the quantities plotted in Figs. 5 and 7 show anomalous behaviors at different temperatures, one at T_g and the other at T_c. At different Q values, different averages of the mean-square displacement of the different atomic species determine the Debye-Waller factor. At relatively high Q, the interference contribution to the structure factor tends go to zero, and the observed effective mean-square displacement becomes simply averaged over all atoms. So one might argue that the intrinsic microscopic dynamics is best characterized by the high-Q limit of the Debye-Waller factor compared to the one measured at the peak of the structure factor.

The behavior shown in Fig. 7 is the first direct observation, to our knowledge, of a potential signature of a critical temperature T_c above T_g, as predicted by MCT theories. In previous work T_c could only be assessed by assuming *a priori* the validity of some MCT predictions (e.g., scaling). Our result is model-independent evidence hinting at the existence of T_c. The temperature T_c can be considered as a signature of some kind of a phase transition, between two phases with different microscopic dynamics. We obtain a critical temperature of 368 ± 5 K from our data. This value is in good agreement with values of the critical temperature obtained for CKN from earlier neutron spin-echo[3] (370 ± 5 K) and time-of-flight[4] (368 ± 5 K) measurements at $Q \simeq 1.7$ Å^{-1} , and from ultrasound measurements (375 ± 5 K) at $Q=0$ obtained by Fuchs, Götze, and Latz.[14]

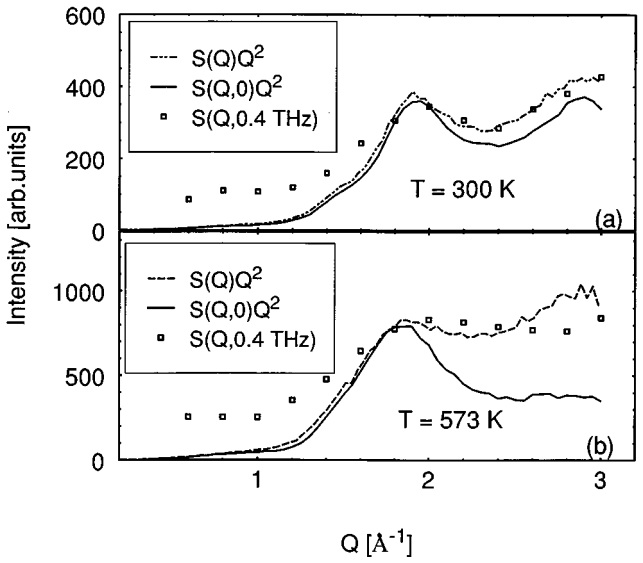

FIG. 12. The inelastic scattering at 0.4 THz (triangles) compared with $Q^2S(Q)$ (dotted line) (Ref. 7), and $Q^2S(Q,\omega=0)$ (solid line) at 300 K (a) and 573 K (b). The data are normalized to give the same height at the main peak.

After removing the temperature dependence of the scattering arising from thermal population effects by dividing by the Bose factor, one obtains the quantity $S_n(Q,\omega,T)$ which is temperature independent for harmonic phonon scattering. Such temperature-independent behavior is essentially what we observe for frequencies larger than 0.5 THz. However, at lower frequencies there is an excess intensity proportional to $(T-T_g)$ that we believe arises from the fast relaxation or β process. The onset of the increase in the inelastic intensity at low frequencies for temperatures above T_g may be regarded as a microscopic dynamic signature of T_g arising from the increased motion and the increase of the mobility of the ions above T_g.[15] The β relaxation is characterized by the same energy dependence of several Q values we studied (Fig. 9). A similar behavior in the frequency region from 0.2 to 0.7 THz has been observed in polymer glasses,[16,17] where the excess intensity is referred to as a boson peak.

The extra intensity at low frequency, $S'(Q,\omega,T)$, has a shape almost the same as that of $S(Q)$. Using a functional form with an excess scattering proportional to the structure factor, Eq. (9), the quantity $b(Q,\omega)$, which reflects the amplitude of the β process, displays a minimum in the region of the peak of $S(Q)$ [Fig. 10(b)]. This form has been predicted within the context of some phenomenological interpretations of the β process as corresponding to a kind of subgroup motion.[1] The remarkable similarity of the Q dependence of $S'(Q,\omega,T)$ to that of $S(Q)$ is very strong evidence in favor of the interpretation of the character of the β process as a

relaxation of the overall atomic short-range structure.[1]

The Q dependence of the inelastic phononlike scattering at constant frequency shows some interesting features. As shown in Fig. 11, a remnant of the main peak of the elastic structure factor is still present at 0.4 THz , but not at higher frequencies. Figure 12 shows that the scattering at low frequency, 0.4 THz, follows $Q^2S(Q)$ behavior for Q values above the main peak, but not at smaller Q values. The excess intensity at smaller Q values probably corresponds to the excess density of low-energy modes (of localized nature) characteristic of amorphous materials.

In this paper we have presented the results of a rather broad study of the neutron scattering by the ionic glass CKN. The work shows the value of such extensive studies for revealing the complex variety of features that glasses can display. By having available neutron-scattering results for both $S(Q)$ (from our previous studies presented elsewhere[7]) and $S(Q,\omega=0)$ one obtains a much more complete picture of the static behavior of both the liquid and glass states. Our work on CKN has extended the knowledge of the behavior of glass materials at temperatures near and above the glass-transition temperature to reveal several puzzling features that are in need of explanation and additional experimental exploration. These include the different behavior of the Debye-Waller factor at different values of Q, the appearance above T_g of an extra scattering intensity scaling with $S(Q)$ below a threshold frequency of about 0.5 THz, and the presence of excess inelastic phonon intensity at low Q. Several aspects of the behavior of CKN revealed by our study support the predictions of mode-coupling theory, while others show serious shortcomings of this theory. Much more work, both experimental and theoretical, needs to be done before we can claim a fundamental understanding of glass-forming systems, and of what happens at T_g and T_c in particular. The present work has shown additional ways in which it will undoubtedly be valuable to proceed in studying other glass-forming systems, as well as indicating several promising ways in which the study of CKN should be extended.

ACKNOWLEDGMENTS

We thank the staff of the Neutron and Condensed Matter Science Branch, Chalk River Laboratories, for help with the performance of the neutron-scattering measurements, and D. C. Tennant for designing the aluminum container. This work was partially supported by the Natural Sciences and Engineering Research Council of Canada.

*On leave from Material Science Research Centre, BATAN, Puspiptek Serpong, Indonesia.

†Present address.

[1] W. Götze, *Liquids, Freezing and the Glass Transition*, edited by D. Levesque, J.P. Hansen, and J. Zinn-Justin (Elsevier, Amsterdam, 1991).

[2] C.A. Angell and E. Williams, J. Phys. Chem. **81**, 232 (1977).

[3] F. Mezei, W. Knaak, and B. Farago, Phys. Rev. Lett. **58**, 571 (1987); Phys. Scr. **19**, 571 (1987).

[4] W. Knaak, F. Mezei, and B. Farago, Europhys. Lett. **7**, 529 (1988).

[5] F. Mezei, J. Non-Cryst. Solids **131**, 317 (1991); J. Phys. (France) IV **C2**, 31 (1992); Ber. Bunsenges. Phys. Chem. **95**, 1118 (1991).

[6] E. Kartini and F. Mezei, Physica B **213&214**, 486 (1995)

[7] E. Kartini, M.F. Collins, B. Collier, F. Mezei, and E.C. Svensson, Can. J. Phys. **73**, 748 (1995).

[8] K.J. Rao, D.B. Helphrey, and C.A. Angell, Phys. Chem. Glasses **14**, 26 (1973).

[9] A. Dietzel and H.P. Poegel (unpublished).

[10] F. Mezei, in *Liquids, Freezing and the Glass Transition*, edited by D. Levesque, J.P. Hansen, and J. Zinn-Justin (Elsevier, Amsterdam, 1991).

[11] J. Wutke, M. Kiebel, E. Bartsch, F. Fujara, W. Petry, and H. Sillescue, Z. Phys. B **91**, 357 (1993)

[12] U. Buchenau, in *Dynamic of Disordered Materials*, edited by D. Richter, A.J. Dianoux, W. Petry, and J. Teixera (Springer-Verlag, Berlin, 1989), p. 172, and references therein.

[13] W. Knaak, in *Dynamic of Disordered Materials* (Ref. 12), p. 64.

[14] M. Fuchs, W. Götze, and A. Latz, Chem. Phys. **149**, 185 (1990).

[15] M.H. Cohen and G.S. Grest, Phys. Rev. B **24**, 4091 (1981).

[16] B. Frick, D. Richter, and B. Farago, J. Non-Cryst. Solids **131-133**, 169 (1991); B. Frick and D. Richter, Phys. Rev. B **47**, 14 795 (1992); B. Frick, D. Richter, R. Zorn, and L.J. Fetters, J. Non-Cryst. Solids **172-173**, 272 (1994).

[17] T. Kanaya, T. Kawaguchi, and K. Kaji, J. Chem. Phys. **98**, 8262 (1993); T. Kawaguchi, T. Kanaya, and K. Kaji, Physica B **213&214**, 510 (1995).